Bull. Mater. Sci., Vol. 36, No. 7, December 2013, pp. 1139–1145. © Indian Academy of Sciences.

# Nanoindentation study on Gd-deposited YBaCuO superconductor

**F YILMAZ[a,*], O UZUN[a], U KOLEMEN[a], M F KILICASLAN[b], N BASMAN[a], S ERGEN[a], K OZTURK[c] and E YANMAZ[c]**

[a]Department of Physics, Faculty of Arts and Science, Gaziosmanpaşa University, Tokat 60240, Turkey
[b]Department of Physics, Faculty of Arts and Science, Kastamonu University, Tokat, Turkey
[c]Department of Physics, Faculty of Arts and Science, Karadeniz Technical University, Trabzon 61080, Turkey

MS received 8 February 2012; revised 24 February 2013

**Abstract.** **Nanoindentation technique was used to characterize the mechanical properties of Gd-deposited bulk YBaCuO superconductors fabricated by solid-state reaction method. In order to determine the hardness and reduced modulus of the samples, load-displacement data were analysed by using the Oliver–Pharr method. The hardness values exhibited significant peak load-dependence especially at lower peak loads, while the reduced modulus values were found to be nearly constant at studied loading range. In order to find true hardness of the samples, the peak load-dependency of hardness was analysed by using Meyer's law, minimum resistance model, elastic/plastic deformation model, energy balance model, Nix–Gao model and Mukhopadhyay approach. Of the aforementioned models, energy balance model and Mukhopadhyay approach were found to be the most effective models to explain the load-dependency of hardness.**

**Keywords.** **YBaCuO superconductor; Gd-deposition; nano-indentation; indentation size effect.**

## 1. Introduction

Since the discovery of superconductivity in YBaCuO (Y123 or YBCO) system, significant progress has been made in the development of samples with high critical current density ($J_c$) and high critical temperature ($T_c$) (Ozturk *et al* 2010; Choi *et al* 2011). For the purpose of enhancing transport and magnetic properties, many investigations have been performed on the flux pinning force in Y123 system. Several studies have shown that flux pinning can be improved through chemical doping with rare-earth elements (Pr, Nd, Sm, Eu, Gd, Er, etc) because of their greater radius than Y, which brings about stronger pinning strength (Farbod and Batvandi 2011). Previously, it has been reported that diffusion doping of Y123 by Gd improved the pinning properties, and increased the critical current density and critical transition temperature compared to pure Y123 (Öztürk *et al* 2007, 2008).

The improvement of mechanical properties such as strength, fracture toughness, hardness ($H$) and reduced modulus ($E_r$) as well as critical current density and critical transition temperature are crucial for many technological applications of superconductors (Katagiri *et al* 2006). That is why, mechanical properties of superconductors need to be improved without loosing their superconducting properties. Accordingly, a number of studies have been carried out recently to improve the mechanical properties of superconductors (Karaca *et al* 2009; Seki *et al* 2010; Elsabawy 2011). Nanoindentation is one of the most efficient techniques to determine the mechanical properties of both bulk solids and thin films (Chawla *et al* 2009; Plummer *et al* 2011). Apart from conventional hardness test, this method is capable of measuring not only hardness ($H$), but also reduced elastic modulus ($E_r$) of the materials. Furthermore, load and displacement (depth) of an indentation are continuously monitored and optical observation and measurement of the diagonal length of the indentation print, which can be difficult to obtain and subjected to inaccuracy are no longer required (Mencik 2006). Recently, Roa *et al* (2011a, b) successfully performed nano-indentation technique to determine the mechanical properties of multilayered epitaxial YBCO thin films and Bridgman YBCO samples, in which crack formations during indentation and load dependency of hardness have been examined in detail (Roa *et al* 2011a, b).

In this research, we have performed nano-indentation technique on YBCO superconductors fabricated by solid-state reaction method and investigated the effect of Gd-diffusion on mechanical properties. Furthermore, the load dependency of hardness has been examined according to the several empirical models proposed in literature to find out the intrinsic reasons responsible for indentation size effect.

## 2. Experimental

### 2.1 *Preparation of samples*

YBaCuO samples were prepared by the solid-state reaction method from high-purity starting powders $Y_2O_3$, $BaCO_3$ and CuO. More detailed information about the preparation

*Author for correspondence (fikretyilmaz79@gmail.com.tr)

**Table 1.** Experimental conditions and sample labels.

| Sample code | Gd-deposition | Annealing time (h) | Annealing temperature (°C) |
|---|---|---|---|
| Y123 | No | 12 | 900 |
| Gd12 | Yes | 12 | |
| Gd96 | Yes | 96 | |

of YBaCuO samples can be found in our previously published papers (Öztürk *et al* 2007, 2008). Gd diffusion in YBaCuO pellets was carried out using an ultra-high vacuum electron-beam deposition system to get a layer of Gd (thickness ∼4 $\mu$m) on one side sample of the surface. The diffusion annealing of samples with the deposited layer of Gd was executed in air at temperature 900 °C for 12 and 96 h. For comparison, a pure YBaCuO uncoated with Gd layer was also annealed at 900 °C for 12 h in air. The experimental conditions and sample labels are listed in table 1.

### 2.2 *Indentation and AFM procedure*

Indentation experiments were conducted with a Berkovich tip using NH–2 nanoindenter (CETR) with load and displacement resolutions of ±0·1 $\mu$N and ±0·02 nm, respectively. Prior to indentation experiments, samples on the mounting stage were adjusted to prevent tilting in $z$-axis. At least ten indents were made for each peak load (10, 50, 100, 200, 300 and 400 mN) at different locations of the samples. The atomic force microscopy measurements were carried out with $Q$-scope series SPM (manufactured by Ambios Technology) attached on a nanoindenter. The images were collected in non-contact mode.

## 3. Results and discussion

Figure 1 shows load-displacement ($P$–$h$) curves of the samples under different peak loads. The loading segments of $P$–$h$ curves are overlapped with each other, which points out a similar deformation mechanism for different loading cycles. The overlapping characteristic of $P$–$h$ curves also implies that all samples have a homogeneous microstructure, which is in agreement with the work previously published by Karaca *et al* (2009).

Oliver–Pharr (O–P) model was utilized to calculate $H$ and $E_r$ of the samples. Detail of the method is described elsewhere (Oliver and Pharr 1992). In order to verify the applicability of this model, it is always necessary to calculate $h_f/h_{max}$ ratio, where $h_{max}$ is the indenter depth at maximum load and $h_f$ the final depth of contact impression after unloading. When $h_f/h_{max}$ is higher than the critical value of 0·7, pile-up is significant, whereas sink-in behaviour is the dominant factor, when $h_f/h_{max}$ is less than 0·7. The value of this ratio should lie below or at least close to 0·7 to obtain reliable results from O–P model (Bolshakov and Pharr 1998). The average values of $h_f/h_{max}$ ratio for the samples were found to be close to the boundary value of 0·7 (figure 2). This information justifies the basic applicability of O–P model to analyse the nano-indentation data in the present study. Also, the inset AFM image in figure 2, clearly shows no pile-up or sink-in around the indent, which is in accordance with the results of $h_f/h_{max}$ value.

Figure 3 shows $H$ values of the samples, where $H$ values decrease with increasing contact depth $h_c$. This phenomenon, which is known as the indentation size effect (ISE), has been reported by the previous studies for YBaCuO samples (Uzun *et al* 2005; Roa *et al* 2011a). ISE is generally explained in terms of a variety of causes, such as work hardened surface layers, hard surface oxides, contaminants, tip bluntness or poor tip-shape calibrations, all of which could result in ISE (Fischer-Cripps 2011). ISE leads to an uncertainty in the determination of true hardness of materials. Therefore, several approaches based on elastic recovery, energy balance, strain gradient plasticity (SGP), surface roughness, friction, etc have been proposed to account for ISE. In the following section, load dependency of hardness observed in this study will be discussed in terms of the well known models presented in literature.

### 3.1 *Analysing of ISE*

ISE has been observed in a wide variety of materials, such as ceramics, metals or intermetallics and various models have been suggested to account for ISE. All these models to some extent had some utility, but they are sometimes failed for the different material groups because of their dissimilar physical or chemical nature. Recently, Mukhopadhyay and Paufler (2006) outlined these models elsewhere. In the following sections, we have applied different models to our data to find the most appropriate model which explains our results well.

3.1a *Meyer's law*: Meyer's law was first developed to determine the work hardening capacity of metals in Brinell hardness test and then it was extended for non-spherical indenters by Onitsch (1947). Meyer's equation or in other words power law equation can be expressed as

$$P = C_1 h_c^n, \tag{1}$$

where $P$ is the applied load, $C_1$ and $n$ are material constants and $h_c$ the indentation contact depth (or indentation diagonal in static hardness test). Figure 4 shows plots of Meyer's equation for ln $P$ and ln $h_c$ values, from which the power law indexes, $n$, were obtained as 1·67, 1·73 and 1·74 for Y123, Gd12 and Gd96, respectively (table 2). When $n$ value is below 2, it shows the presence of ISE. On the other hand, according to Onitsch (1947), $n$ should lie between 1 and 1·6 for hard materials and higher than 1·6 for soft materials. In this study, all $n$ values are above the critical value of 1·6, which seems meaningless for our samples

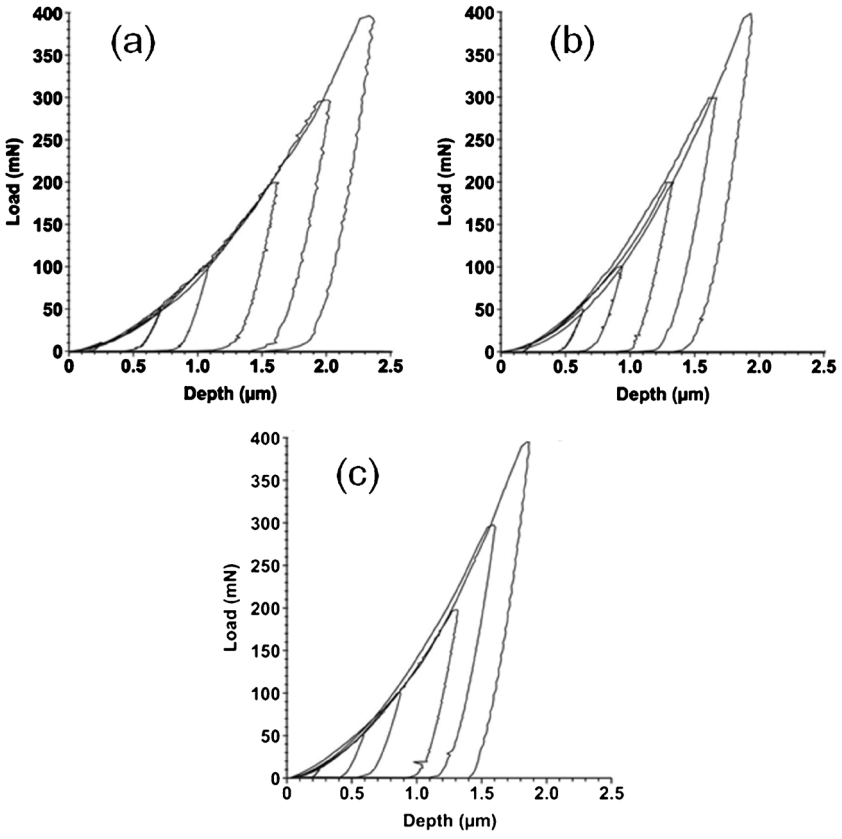


**Figure 1.** *P–h* curves of **(a)** Y123, **(b)** Gd12 and **(c)** Gd96.

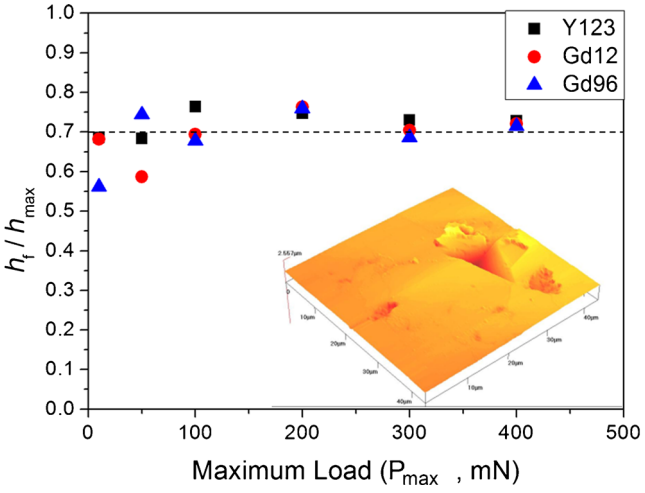


**Figure 2.** Ratio of $h_f$ /$h_{max}$ for samples at loading range of 10–400 mN. Inset picture shows AFM image of an indent for peak load of 400 mN.

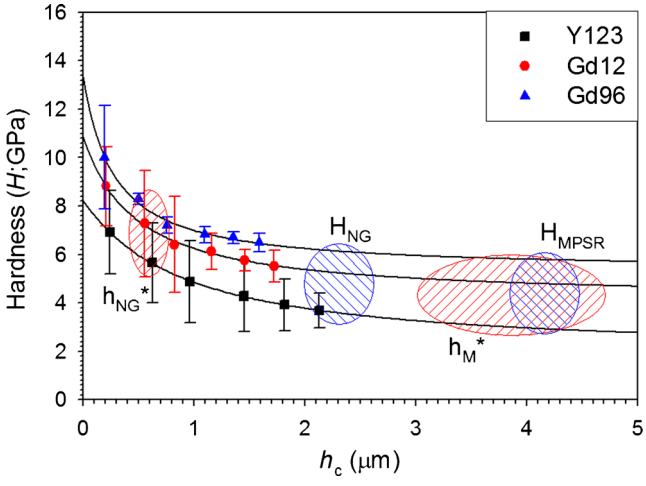


**Figure 3.** Variation of hardness with contact depth ($h_c$).

because of the hard nature of YBCO superconductor. Moreover, Meyer's law is unable to determine the true hardness as it is continuously decreasing with applied load.

3.1b *Hays–Kendall model: minimum resistance model*: Hays and Kendall (1972) have put forward an idea that there is a minimum resistance on the surface and if the applied load exceeds this resistance, plastic deformation occurs, otherwise the deformation is only elastic. According to this model, the load–displacement relation can be expressed as

$$P = W + C_2 h_c^2, \tag{2}$$

where $C_2$ is a constant independent of load and $W$ a minimum load necessary to initiate plastic deformation. $W$ and

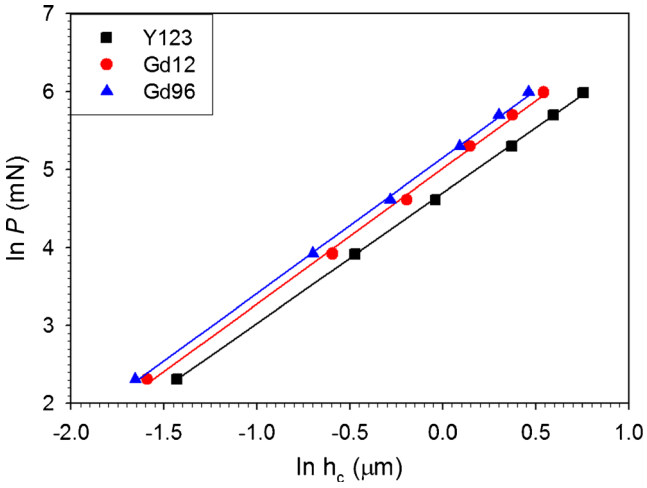


**Figure 4.** Plots of ln $P$ vs ln $h_c$ according to Meyer's law.

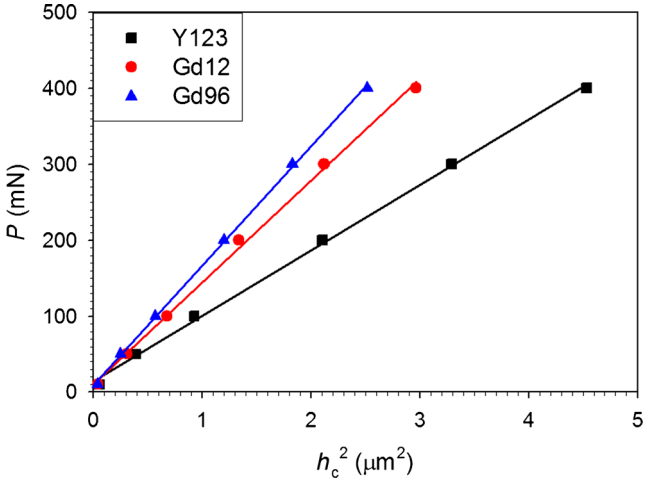


**Figure 5.** Plots of $P$ vs $h_c^2$ according to Hays–Kendall model.

$C_2$ can be obtained from the intersection of the linear plot of $P$ vs $h_c^2$. Therefore, load-independent hardness can be expressed as

$$H_{HK} = kC_2, \tag{3}$$

where $k$ is the indenter shape factor, 0·0408 for Berkovich tip. Figure 5 shows plots obtained by the fitting of (2). $W$ and $C_2$ parameters are summarized in table 2. The correlation coefficients were found to be 0·99, implying that (2) provides a satisfactory description of data for the samples. The minimum loads for plastic deformation ($W$) were predicted to be 14·6, 10·1 and 9·48 mN for Y123, Gd12 and Gd96, respectively. An additional indentation test was conducted for the sample Y123 to know whether the predicted $W$ value is true. It is clearly seen in figure 6 that even though we applied a lower load than $W$ for Y123 sample, the loading and unloading curves are well separated, indicating that there was a permanent deformation during indentation. Therefore, minimum load required for the permanent deformation predicted

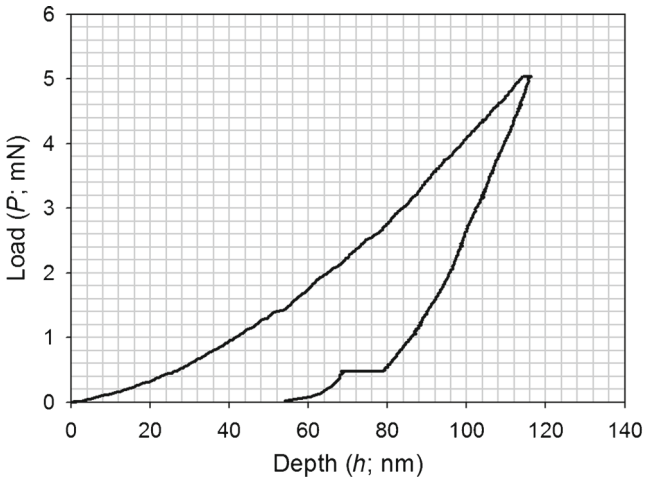


**Figure 6.** $P$–$h$ curve obtained from Y123 sample under a peak load of 5 mN shows a permanent deformation.

by the minimum resistance model is too large to be accepted, invalidating the applicability of this approach for analysing ISE.

3.1c *Elastic/plastic deformation model*: Bull *et al* (1989) proposed a quantitative model to explain ISE, which is applicable to hard brittle materials, where the elastic deformation effect is significant. Considering this effect, it was suggested that the measured indentation size had to be corrected with a revised term in order to obtain the load-independent hardness

$$H_{EP} = k\frac{P}{(h_c + h_0)^2}, \tag{4}$$

where $k$ is the indenter shape factor and $h_0$ the correction term. The correction term should be positive due to the elastic recovery, which results in a shortage in indentation size. To analyse the indentation data, (4) may be rearranged as follows:

$$P^{1/2} = \kappa^{1/2}h_c + \kappa^{1/2}h_0, \tag{5}$$

where $\kappa = H_{EP}/k$ is a parameter related to the load-independent hardness ($H_{EP}$) and can be directly used for the calculation of $H_{EP}$. Figure 7 shows plots of $P^{1/2}$ against $h_c$ and the obtained best-fit values of $\kappa$ and $h_0$ are listed in table 2. All data points in figure 7 show a linearity with a very high correlation coefficients, $r^2 = 0{\cdot}999$. However, the estimated correction terms, $h_0$, for all samples are comparable with the contact depth, $h_c$, especially at low loads. In other words, $h_0$ values are too large to be accepted. This result shows that elastic/plastic deformation model is also inadequate to explain ISE observed in these samples.

3.1d *Nix–Gao model*: Nix and Gao (1998) proposed a model to explain ISE, which was based on geometrically necessary dislocations (GNDs). For a geometrically

**Table 2.** Best-fit results of the parameters in (1), (2) and (5).

| Sample | $n$ | $C_1$ (mN/$\mu$m$^n$) | $W$ (mN) | $C_2$ (mN/$\mu$m$^2$) | $h_0$ ($\mu$m$^2$) | $\chi$ (mN/$\mu$m$^2$) |
|---|---|---|---|---|---|---|
| Y123 | 1·67 | 110 | 14·6 | 86·1 | 0·153 | 77·6 |
| Gd12 | 1·73 | 150 | 10·1 | 134 | 0·080 | 125 |
| Gd96 | 1·74 | 172 | 9·48 | 157 | 0·079 | 145 |

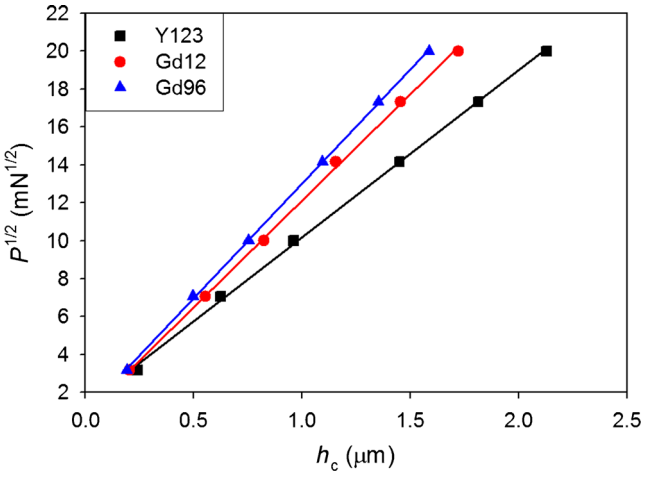


**Figure 7.** Plots of $P^{1/2}$ vs $h_c$ according to elastic/plastic deformation model.

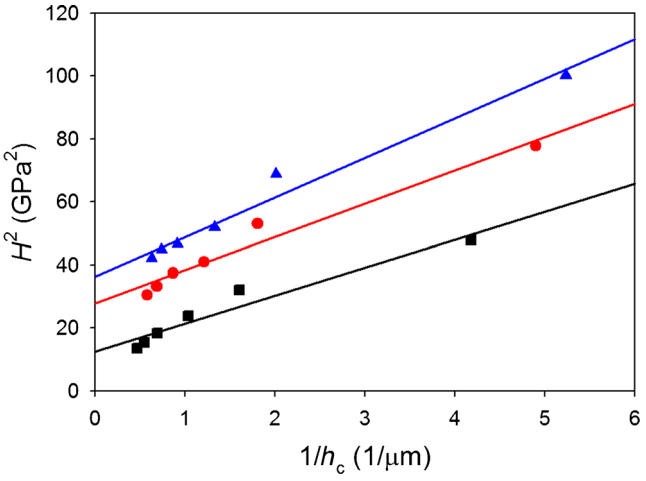


**Figure 8.** Plots of $H^2$ vs $1/h_c$ according to Nix–Gao model.

similar indenter, load dependency of hardness can be formulated through the following equation

$$\frac{H}{H_0} = \sqrt{1 + \frac{h_{NG}*}{h_c}}, \tag{6}$$

where $H$ is the nominal hardness for a given depth and $h_{NG}*$ the characteristic depth that depends on the shape of indenter and the material. True hardness, $H_0$, can be defined as the hardness that would arise from the statistically stored dislocations alone. By using (6), the square of hardness values was plotted as a function of the reciprocal of the indentation depth (figure 8). All data points show a relatively low correlation coefficient, $r^2 = 0{\cdot}9$, compared to the other models. Fitting parameters are listed in table 3. It is clearly seen from figure 3, that $h_{NG}*$ values are in load-dependent region, so this model cannot be used to characterize the load-independent behaviour of the samples. Moreover, due to the fact that the covalent bonding in YBCO materials makes the dislocations immobile, Nix–Gao model, based on dislocation movement, is not convenient to explain ISE in YBCO samples.

3.1e *Energy balance model: modified proportional specimen resistance (MPSR)*: Gong *et al* (1999) proposed an energy balance model for analysing ISE and for determining true hardness. The corresponding equation can be expressed as:

$$P = a + bh_c + ch_c^2, \tag{7}$$

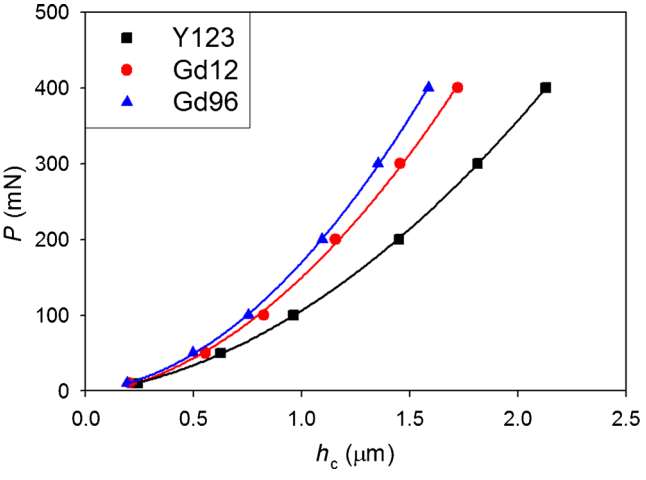


**Figure 9.** Plots of $P$ vs $h_c$ according to energy balance model.

where $a$ is a measure of the surface residual stress associated with surface polishing, $b$ and $c$ are related to the elastic and plastic properties of the test material, respectively. According to this model, $c$ parameter is a measure of true hardness. $a$, $b$ and $c$ parameters can be estimated by plotting $P$ vs $h_c$ as shown in figure 9. The highest correlation coefficient, $r^2 = 0{\cdot}9999$, was obtained for each samples. The estimated fitting parameters are listed in table 3.

True hardness values of samples calculated by using the aforementioned models are summarized in table 4. The plateau hardness values given in table 4, representing load-independent hardness region, were estimated from figure 3.

**Table 3.** Best-fit results of the parameters in (6), (7) and (8).

| Sample code | $h_{NG}$* ($\mu$m) | $h_M$* ($\mu$m) | $a$ (N) | $b$ (N/m) | $c$ (N/m$^2$) |
|---|---|---|---|---|---|
| Y123 | 0·843 | 4·67 | −2·22 | 37·5 | 71·1 |
| Gd12 | 0·618 | 4·12 | −5·78 | 42·0 | 113 |
| Gd96 | 0·588 | 3·01 | −0·78 | 29·9 | 141 |

**Table 4.** True hardness values obtained from the models.

| Sample code | True hardness according to the models (GPa) | | | | Plateau hardness values |
|---|---|---|---|---|---|
| | Minumum resistance | Elastic–plastic deformation | Nix–Gao | Energy balance | |
| Y123 | 3·51 | 3·17 | 3·54 | 2·90 | 3·10 |
| Gd12 | 5·48 | 5·12 | 5·26 | 4·64 | 4·80 |
| Gd96 | 6·41 | 5·93 | 6·02 | 5·76 | 5·85 |

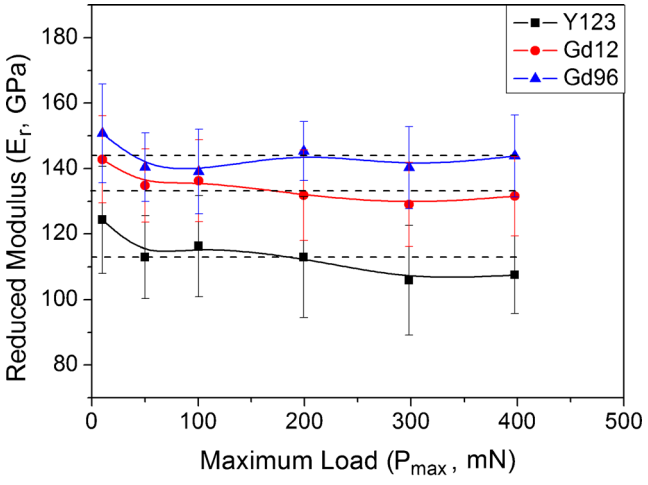


**Figure 10.** Variation of $E_r$ with maximum loads.

As can be seen in table 3,hardness values calculated via energy balance model are closer to the plateau values than those estimated by other models.

3.1f *Mukhopadhyay approach: combined approach*: Recently, Mukhopadhyay (2005) combined the energy balance model and the Meyer's law in order to find the critical indentation size which is related to the upper bound of ISE. The critical indentation size has the same meaning of characteristic depth given in Nix–Gao model. The critical indentation size, $h_M$*, can be formulated as

$$h_{M^*} = \left(\frac{C_1 s^2}{c}\right)^{\frac{1}{2-n}} = \left(\frac{C_1}{c}\right)^{\frac{1}{2-n}} \text{in } \mu\text{m as } s = 1\ \mu\text{m}, \quad (8)$$

where $C_1$ and $n$ are the same parameters as given in (1) and $c$ the same parameter as given in (7). This is a significant relation, which connects with the Meyer's equation to the energy balance model.

The critical indentation size for each sample was determined according to the Mukhopadhyay approach and given in table 3. These values appear to be reasonable and consistent with the trend of hardness plot with the indentation size. It is clearly seen in figure 3 that while the characteristic depths ($h_{NG}$*) estimated from Nix–Gao model are in load-dependent hardness region, critical indentation sizes ($h_M$*) estimated from Mukhopadhyay approach are in load-independent hardness region. This result demonstrates that Mukhopadhyay approach can better predict the critical indentation size after which ISE does not exist.

The obtained true hardness values (table 4) indicate that Gd-diffusion increased the hardness of YBCO superconductor dramatically. It is well known that solute addition in metals and ceramics can increase mechanical strength in terms of substitutional solid-solution mechanism. Öztürk *et al* (2007) observed no secondary Gd phase in Gd-diffused YBaCuO samples (at 900 °C for 12 h) but they found an increase in $c$ lattice parameter, which implied that Y atoms were partly substituted by Gd atoms. Gd96 was found to be slightly harder than Gd12. This is because the longer annealing time can eliminate pores and improve the bonding force between the superconducting grains (Khalil and Sedky 2005; Nursoy *et al* 2008).

The reduced modulus ($E_r$) of the samples vs maximum load is depicted in figure 10. Since $E_r$ is an intrinsic material property and fundamentally related to atomic bonding, the measured reduced modulus is expected to be constant with indentation depth (or load). The results show a small deviation from the expected value at the load of 10 mN. The discrepancy between the expected and obtained results at shallow indentation depths may be due to the effect of polishing. The dashed lines presented in figure 5 shows average $E_r$ values, which are found to be 114, 134 and 144 GPa for Y123, Gd12 and Gd96 samples, respectively. The obtained $E_r$ values are in good agreement with literature values for YBCO (Johansen 2000; Roa *et al* 2011a). Similar tendency was observed for $E_r$ values of the samples as in $H$ values.

Typically, $E_r$ is directly proportional to $H$, which is also observed in many kinds of materials.

## 4. Conclusions

Nano-indentation technique has been used to determine the mechanical properties of Gd-diffused YBCO superconductors. From the above observation, the following conclusions can be drawn:

(I) The overlapping characteristic of $P$–$h$ curves indicates that the samples have a similar deformation mechanism for different loading cycles.
(II) $h_f$ /$h_{max}$ ratio for all samples was found to be close to 0·7, which indicates that neither pile-up nor sink-in is significant. This information justified the basic applicability of the O–P model to calculate $H$ and $E_r$ of the samples.
(III) Hardness values exhibited load-dependent behaviour (ISE), viz. the measured hardness values increase with decreasing indentation depth. ISE behaviour has been analysed by using some empirical models.
(IV) Meyer's law is sufficient for the description of the experimental data but inadequate to determine the true hardness as it is continuously decreasing with applied load.
(V) The minimum load required for permanent deformation predicted by the Hays–Kendal model is too large to be accepted, invalidating the applicability of this approach for analysing ISE.
(VI) The elastic/plastic model is inadequate to explain ISE because the estimated correction term $h_0$, is comparable with the contact depth, $h_c$, especially at lower loads.
(VII) The characteristic depth, $h_{NG}$*, calculated via Nix–Gao model is too small to characterize the load-independent behaviour.
(VIII) The calculated true hardness values by energy balance model are more convenient than those obtained by other models.
(IX) The critical indentation size ($h_M$*) estimated from Mukhopadhyay approach is more reasonable than $h_{NG}$* and consistent with the trend of the hardness plot with the indentation size.
(X) From the nano-indentation experiments, we have found that while Gd-diffusion markedly increases the hardness and elastic modulus of YBCO, longer annealing time slightly increases these properties.

## Acknowledgments

The authors would like to acknowledge the financial support (Project No. 2003K120510) by Turkish State Planning Organization (DPT).

## References

Bolshakov A and Pharr G M 1998 *J. Mater. Res.* **13** 1049
Bull S J, Page T F and Yoffe E H 1989 *Philos. Mag. Lett.* **59** 281
Chawla V, Jayaganthan R and Chandra R 2009 *Bull. Mater. Sci.* **32** 117
Choi K Y, Jo I S, Han S C, Han Y H, Sung T H, Jung M H, Park G S and Lee S I 2011 *Curr. Appl. Phys.* **11**, 1020
Elsabawy K M 2011 *Cryogenics* **51** 452
Farbod M and Batvandi M R 2011 *Physica C* **471** 112
Fischer-Cripps A C 2011. *Nano-indentation* (New York: Springer) 3rd ed., **361** p. 91
Gong J H, Wu J J and Guan Z D 1999 *J. Eur. Ceram. Soc.* **19** 2625
Hays C and Kendall E G 1972 *Metall.* **6** 275
Johansen T H 2000 *Supercond. Sci. Technol.* **13** 121
Karaca I, Uzun O, Kolemen U, Yılmaz F and Sahin O 2009 *J. Alloys Compd.* **476** 486
Katagiri K, Hatakeyama Y, Sato T, Kasaba K, Shoji Y, Murakami A, Teshima H and Hirano H 2006 *Physica C* **445–448** 431
Khalil S M and Sedky A 2005 *Physica B* **357** 299
Mencik J 2006 *Meccanica* **42** 19
Mukhopadhyay N K 2005 *J. Mater. Sci.* **40** 241
Mukhopadhyay N K and Paufler P 2006 *Int. Mater. Rev.* **51** 209
Nix W D and Gao H 1998 *J. Mech. Phys. Solids* **46** 411
Nursoy M, Yılmazlar M, Terzioğlu C and Belenli I 2008 *J. Alloys Compd.* **459** 399
Oliver W C and Pharr G M 1992 *J. Mater. Res.* **7** 1564
Onitsch E M 1947 *Mikroskopie* **2** 131
Öztürk K, Çelik Ş, Çevik U and Yanmaz E 2007 *J. Alloys Compd.* **433** 46
Öztürk K, Çelik Ş and Yanmaz E 2008 *J. Alloys Compd.* **462** 19
Ozturk A, Duzgun I and Celebi S 2010 *J. Alloys Compd.* **495** 104
Plummer J D, Goodall R, Figueroa I A and Todd I 2011 *J. Non-Cryst. Solids* **357** 814
Roa J J, Konstantopoulou K, Jimenez-Pique E, Martin V, Segarra M and Pastor J Y 2011a *Ceram. Int.* doi:10.1016/j.ceramint.2011.10.039
Roa J J, Jimenez-Pique E, Puig T, Obradors X and Segarrra M 2011b *Thin Solid Films* **519** 2470
Seki H, Wongsatanawarid A, Kobayashi S, Ikeda Y and Murakami M 2010 *Physica C* **470** 1177
Uzun O, Kölemen U, Çelebi S and Güçlü N 2005 *J. Eur. Ceram. Soc.* **25** 969